Mansoura Engineering Journal

Volume 19 | Issue 3 Article 1

9-1-2021

Prediction of Film Cooling Effectiveness by a Row of Moles over a Flat Surface.

Handry Ammari
Mechanical Engineering Department., Mu'tah University., Jordan.

N. Hay
Mechanical Engineering Department., University of Nottingham., UK.

Mansoura Engineering Journal, Vol. 19, No.3, September 1994 M,27

PREDICTION OF FILM COOLING EFFECTIVENESS BY A ROW OF HOLES OVER A FLAT SURFACE

H. AMMARI
Department of Mechanical Engineering
Mu'tah University, JORDAN

N. HAY
Department of Mechanical Engineering
University of Nottingham, UK.

تقدير فعالية التبريد الطبقي الناتج عن الحقن من صف عرضي من الثقوب في سطح مستوى بطريقة عدديه

الخلاصه:

بحث هذا البحث طريقه عدديه ويبين قدرتها على حساب فعالية التبريد الطبقي الناتج عن الحقن من صف عرضي من الثقوب في سطح مستوى . وقد تم الاخذ بعين الاعتبار طبيعة الجريان الدوراني في منطقة ما بعد الحقن ، ومحاكاه تأثير الاضطراب باستخدام نموذج الاضطراب k-ε . وقد استخلصت النتائج تحت ظروف العوامل التالية : زاويتي حقن ٣٥° و ٩٠° ، والمسافة بين الثقوب المتجاوره بقدر ٣ أضعاف قطر الثقب ، ونسبة كثافة غاز التبريد الى الغاز الرئيس بمقدار ١,٠ و ٢,٠ ، ومعدل جريان غاز التبريد الى الغاز الرئيس من ٥,٠ الى ٢,٠ . وبمقارنة فعالية التبريد الطبقي المحسوبة عدديا مع مثيلتها المحسوبة مخبريا أظهرت النتائج مطابقة جيده بينهما بصورة عامه .

ABSTRACT

The present paper describes a numerical procedure and its capability for calculating the film cooling effectiveness by injection from a single transverse row of discrete holes over a flat surface. The three-dimensional calculation procedure takes into account the elliptic nature of the flow after the injection. The effects of turbulence are simulated through the implementation of the standard k-ε turbulence model. Results are given for; two injection angles of 35° and 90°, spacing between the holes of 3 hole diameters, coolant-to-mainstream density ratios of 1.0 and 2.0, and blowing rates from 0.5-2.0. The predicted cooling effectiveness is compared with some available experimental data and shows an overall performance of reasonably good agreement.

INTRODUCTION

Discrete hole film cooling is used extensively on turbine blades and vanes to protect the surface of the blades and vanes from the high temperature combustion gas. Coolant from the relatively cooler compressor air is bypassed to the cooling system, in which it is dumped through the surface of the blades into the external boundary layer in order to form a protecting blanket on the blade surface. The injected coolant lowers the temperature near the surface through mixing with the boundary layer fluid.

The film cooling process is characterized by the heat transfer coefficient and the adiabatic wall temperature T_{aw} represented by the adiabatic wall effectiveness,

$$\eta_{aw} = (T_\infty - T_{aw})/(T_\infty - T_c)$$

where T_∞ and T_c are the mainstream gas and the coolant temperatures respectively.

Received 17 th. May, 1994.

If a mass transfer process is used, an adiabatic wall is represented by an impermeable one. Thus, the equivalent to the adiabatic wall effectiveness η_{aw} is the impermeable wall effectiveness η_{iw} given in terms of the mass concentration of coolant gas, c_{iw}, at an impermeable wall as follows:

$$\eta_{iw} = c_{iw}$$

Design considerations has forced engineers to inject the coolant through discrete holes rather than through slots. The injected air through holes generates a complex three-dimensional flow field with flow reversal near the injection when it interacts with the oncoming mainstream [1], which is basically two-dimensional. The main parameters influencing the spreading of the coolant and hence the film cooling effectiveness are the injection angle α, the hole spacing s/D, and the blowing rate $M=\rho_c u_c/\rho_\infty u_\infty$, apart from the hydrodynamic state of the coolant, mainstream pressure gradient and turbulence intensity, and surface curvature.

Experimental studies of the dependence of the film cooling process on these parameters for optimization of the film cooling design of gas turbine blades are necessary. However, experimental parameter investigations are very expensive under typical engine conditions. Therefore, designers are in great need for prediction procedures.

Accurate analysis of the flowfield in the vicinity of injection through discrete holes requires three-dimensional calculation procedures. Patankar et al [2] analyzed the injection at high blowing rates from a single normal hole. Their numerical calculation was based on three-dimensional elliptic finite-difference scheme. Bergeles et al [3] calculated laminar flow and temperature fields for injection via a single and multi-row of holes inclined at 90°, 45° and 35° by applying a partially parabolic calculation code. They have also considered a case for which injection was through a row of holes at 30° in the presence of density gradients and strong mainstream acceleration. Their predictions of the spanwise averaged effectiveness for the latter case agreed satisfactorily with some experimental data. Further, in another two publications, Bergeles et al [4, 5] predicted the film cooling effectiveness for injection through a row and two rows of holes aligned at 30° to a turbulent mainflow. The numerical simulation method presented embodied a semi-elliptic treatment of the flowfield in the vicinity of the holes. The most widely used k-ε two-equation model of turbulence, which assumes an isotropic eddy viscosity, was modified by introducing non-isotropic transport coefficients. The numerical results showed a good agreement for the cases of low blowing rates ($M<0.5$). However, the assumptions of symmetrical jet exit conditions, local equilibrium inherent in the turbulence model, and the inability of the semi-elliptic procedure to properly simulate the zone of recirculation downstream of a hole, has produced significant errors at conditions of small boundary layer thickness and large blowing rates.

Miller and Crawford [6] used an injection model in which the additional lateral mixing was modelled by augmentation of the mixing length in their turbulence model. They have presented predictions of Stanton number and effectiveness for geometries incorporating single, double and multiple rows of holes. They obtained good agreement with experimental data for $M<1.0$ and $\alpha<45°$.

Demuren, Rodi and Schonung [7] employed a locally elliptic calculation procedure, which could be safely applied to regions with flow reversals even at large M. The standard k-ε turbulence model was used but modified as in [4] to account for non-isotropic eddy viscosities and diffusivities. They analyzed the influence of injection angle, relative hole spacing and blowing rate on the effectiveness. Agreement of the effectiveness predictions with systematic data was satisfactory for M up to 1.0 and for small hole spacing, but for high M and large spacing the predicted level of effectiveness was lower than the experimental results.

They claimed that the mixing process was crudely simulated with the turbulence model used.

Tafti and Yavuzkurt [8] developed an injection model and used it with a low Reynolds number k-ε model boundary layer code. The effect of three-dimensional entrainment is introduced in the two-dimensional prediction scheme by using an "entrainment fraction" and an "entrainment enthalpy". The numerical scheme was applied to predict the film cooling effectiveness by injection from a row of holes into a turbulent boundary layer. The predictions of the effectiveness were shown to be in good agreement with experimental data for most of the cases tested.

The aim of this study has been to investigate the ability of a numerical procedure to predict the film cooling effectiveness by a row of holes over flat plates. Comparisons of the computed results with the corresponding experimental data [9, 10, 11] are made to assess the accuracy of the scheme and to explore its use as a design tool for film cooling analysis.

DESCRIPTION OF COMPUTER SCHEME

The computer scheme used, called Phoenics, is a computational-fluid-dynamics program designed for simulating fluid flow, heat transfer, chemical reaction and combustion process. Phoenics was created by CHAM Ltd, UK.

Phoenics version 1.4 was used in this study. This version is installed on the University of Nottingham VAX 11/780 system.

Full description of the main features of Phoenics is provided in reference [12]. Phoenics comprises two essential computer codes and two auxiliary ones. The essential ones are a program supplying problem-defining data and a program containing the main flow-simulating procedure, which incorporates the coding sequences representing the relevant laws of physics. The auxiliary ones are a program that displays the results graphically, and a program which contains extensive instructional material.

The program solves the discretized versions of the well established differential equations expressing the physical laws of conservation of mass, momentum and energy (or species concentration). The equations of continuity, momentum, and energy describing a steady, three-dimensional turbulent flow may be written in Cartesian tensor notation as:

$$\frac{\partial}{\partial x_i}(\rho u_i) = 0$$

$$\frac{\partial}{\partial x_j}(\rho u_i u_j) = -\frac{\partial P}{\partial x_i} + \frac{\partial}{\partial x_j}\left[\mu\left[\frac{\partial u_i}{\partial x_j} + \frac{\partial u_j}{\partial x_i}\right] - \rho\overline{u'_i u'_j}\right]$$

$$\frac{\partial}{\partial x_j}(\rho u_j c) = \frac{\partial}{\partial x_j}\left[\Gamma\frac{\partial c}{\partial x_j} - \rho\overline{u_j c'}\right]$$

where c denotes temperature or species concentration, u'and c' instantaneous velocity and temperature (or species) fluctuations about the mean, respectively, μ and Γ are the dynamic viscosity and diffusivity of the fluid, respectively, and the overbars imply the usual Reynolds averaging.

The equations are solved by a "finite-volume" method involving integration over the grid cells of a calculation domain, followed by iterative solutions of the resulting non-linear algebraic equations. A general description of the solution of the differential equations of conservation is provided in [13]. However, the molecular transport terms in these equations have been neglected in the solution procedure as they are important only in the viscous sublayer very near walls, and this layer is

not resolved in the present calculation but bridged by wall functions as described in the following section.

MATHEMATICAL AND PHYSICAL MODELS

The turbulence time-averaged properties (turbulent shear stresses and heat fluxes) are determined by "turbulence models". The most widely used and accepted model known as the "k-ε" turbulence model is implemented in Phoenics. The model utilises the eddy (turbulent) viscosity concept and calculates two quantities k, the kinetic energy of turbulence and ε, its dissipation rate.

The eddy viscosity, μ_t, is related to the turbulent kinetic energy k and to its rate of dissipation ε through the Kolmogorov-Prandtl relation as,

$$\mu_t = 0.09\ \rho\ k^2 / \varepsilon$$

and the effective viscosity, represented by μ_{eff}, was calculated by,

$$\mu_{eff} = \mu + \mu_t$$

The distribution of k and ε over the flow field is determined from the basic k-ε turbulence model semi-empirical transport equations as given by Launder and Spalding [14] in Cartesian tensor notation:

$$u_i \frac{\partial k}{\partial x_i} = \frac{\partial}{\rho \partial x_i}\left[\frac{\mu_t}{\sigma_k}\frac{\partial k}{\partial x_i}\right] + \frac{\mu_t}{\rho}\left[\frac{\partial u_i}{\partial x_j} + \frac{\partial u_j}{\partial x_i}\right]\frac{\partial u_i}{\partial x_j} - \varepsilon$$

$$u_i \frac{\partial \varepsilon}{\partial x_i} = \frac{\partial}{\rho \partial x_i}\left[\frac{\mu_t}{\sigma_\varepsilon}\frac{\partial \varepsilon}{\partial x_i}\right] + \frac{C_1 \varepsilon \mu_t}{k\rho}\left[\frac{\partial u_i}{\partial x_j} + \frac{\partial u_j}{\partial x_i}\right]\frac{\partial u_i}{\partial x_j} - \frac{C_2 \varepsilon^2}{\rho k}$$

For fully developed turbulent flows, the empirical constants appearing in this standard k-ε model take these values,

$C_1 = 1.44$, $C_2 = 1.92$, $\sigma_k = 1.0$, $\sigma_\varepsilon = 1.3$

The standard k-ε model, however, is valid only for fully turbulent flows where viscous diffusions are neglected, and adopts an isotropic turbulent viscosity.

As viscous diffusions are neglected, the k-ε model is used in conjunction with empirical wall functions to bridge the viscous sublayer. This is accomplished by relating the velocity components at the first grid node outside this layer to the wall shear stress via the logarithmic law of the wall. A uniform shear stress prevails in this viscous layer, and generation and dissipation of energy are in balance there via the assumption that the turbulence is in a state of equilibrium.

The methods which include integration right up to the wall are better than those assuming the wall functions [15] since they are valid throughout the fully turbulent, semilaminar and laminar regions. However, the computing time is increased considerably due to the fine mesh required to resolve the immediate near-wall region adequately. Wall functions economize computer time and storage.

The standard wall-function for turbulent flows is, namely, the logarithmic law,

$$C_f = [k_\nu / \ln(E\ Re\ C_f^{0.5})]^2, \text{ for } Re > 132.5$$

$$C_f = 1 / Re \text{ , otherwise.}$$

where C_f is the skin-friction factor ($=\gamma_w/\rho u^2$, γ_w is the wall shear stress and u is the velocity parallel to the wall), k_ν is the Von Karman constant, taken to be 0.435, and E is the smooth-wall value of 9.0. The Reynolds number, Re ($=uy/\nu_l$), is based on the resultant velocity parallel to the wall, on the distance from the wall to the grid node, y, and on the laminar kinematic viscosity, ν_l. The limit of Re of 132.5 is that at which the laminar and turbulent wall-functions intersect.

The near-wall grid node values of k and ε are fixed to the following empirical correlations via the incorporated logarithmic-law option applicable to smooth walls,

$k_w = u_\tau^2 / 0.3$, and

$\varepsilon_w = u_\tau^3 / (k_w\, y) = 0.09^{3/4}\, k_w^{3/2} / (k_w\, y)$

where, u_τ is the friction velocity ($=(\gamma_w/\rho)^{1/2}=uC_\varepsilon^{1/2}$).

The partial differential equations were solved by a three-dimensional and elliptic calculation procedure to simulate realistically the complex three-dimensional flow near injection and the associated heat transfer processes.

THE PROBLEMS SIMULATED

The physical problems concern film cooling by injection from a single row of 90° or 35° holes of s/D of 3 across a flat plate exposed to a mainstream. The cooling effectiveness is investigated for different blowing rates and density ratios. Examples of the computed results are presented and compared with the available experimental data.

COMPUTATIONAL DETAILS

Geometry and Grid: Three-dimensional computational grids in Cartesian coordinates were employed. The z-direction was taken as that of the mainstream for all of the computations performed. The bottom side of the rectangular-box shaped domains was considered solid, the other sides were all fluid as illustrated in Fig. 1. The lateral boundaries were 1.5D apart, where D is the hole diameter, and located at planes of symmetry; one bisecting a hole, and the other bisecting the space to its neighbour. The solid wall region in the vertical extent (y-direction) was placed to occupy 2D so that the effect of the mainstream on the jet inside the hole was accounted for. The other boundary of the y-direction was adjusted to 6D above the wall surface, just sufficiently to encompass the region of undisturbed flow, so that uniform mainstream conditions were assumed there.

The domain extended upstream some 3D from a hole origin where the oncoming flow was undisturbed by injection. The position of the downstream boundary from the hole origin was adjusted so that z = 46D.

The number of grid nodes used in the x, y and z-directions were 9, 15 and 30 respectively. Fine-grid spacing near a hole was employed and gradually increased for locations away from it so as to give a good resolution of the solution in the area of interest, see Fig. 1. The first grid node away from the wall was chosen that it sufficiently bypassed the viscous sub-layer as required by the wall-functions. This was based on calculations using an established sub-layer thickness relation expressed in terms of the Reynolds number values used as input.

One half of the circular injection hole was included in the domain and was represented by 18 cells in cross-section. The circular shape of the hole inside the wall was specified by fractional volume and area porosities, thus determining the proportion of the hole periphery in each cell open for flow.

Boundary and Initial Conditions: At the mainstream inlet, part of the plane above the wall started with a turbulent boundary layer characterised by the seventh power law. The boundary layer thickness, δ, was set analogous to that in the corresponding experimental situation. Initial profiles were prescribed for the following,

- the mean velocity, $w = w_- (y/\delta)^{1/7}$

where, w is the oncoming air streamwise z-direction velocity, w_- is the free stream conditions velocity, and y is the vertical distance from the wall, and

- the turbulence kinetic energy, k, and dissipation rate, ε, through the following empirical profile [12],

$$k = k_w - 3k_w(y/\delta)^2 + 2k_w(y/\delta)^3$$

$$\varepsilon = 0.09^{3/4}\, k^{3/2} / (k_w\, y)$$

where k_w is k at the wall.

For $y > \delta$, uniform mainstream conditions were set.

The injection velocity, u_c, at the hole entry was specified analogous to the corresponding experimental value, however, the turbulence quantities, k and ε, at the hole entry were given by [12],

$$k = 0.005\, u_c^2, \text{ and}$$

$$\varepsilon = 0.09^{3/4}\, k^{3/2}/(D/2)$$

Iteration Control and Convergence: Convergence was procured within 120 iteration sweeps. The calculations took 60 to 90 minutes CPU time on the VAX. At this stage, velocities, mass fractions and pressure were invariant to within 1%. The sum of the absolute mass errors was less than 1% of the total mass flow rate.

DISCUSSION OF RESULTS

Comparison of the predicted effectiveness is made with experimental data at zero mainstream pressure gradient. The experiments of Goldstein et al [9] and Pedersen et al [10] provided the data for testing the simulations of the laterally averaged and local adiabatic wall effectiveness for injection through a row of 35° holes. The former measured the effectiveness by heating the injectant and surveying the surface temperature, while the latter measured the surface concentration of a foreign gas introduced into the injectant. For the case of normal injection, the measurements of surface concentrations by Foster [11] provided the effectiveness data. The effectiveness could be predicted by calculating either the adiabatic temperature or the mass fraction of the injectant at the wall. Preliminary tests have shown that there was little difference (<5%) between the effectiveness values predicted by the two methods. Here, however, the predicted effectiveness data was based on the mass fractions of the injectant at the wall.

The experimental conditions of reference [9], which were: s/D=3, α=35°, u_∞=30.5m/s, $\bar{\delta}$/D=0.124, Re_D=2.2x10⁴, Tu=0.5% and ρ_c/ρ_∞=0.85, were approximately simulated in the computer program for the inclined injection cases, and those of Foster [11]: s/D=3, α=90°, u_∞=30.5m/s, $\bar{\delta}$/D=0.33, Re_D=0.45x10⁴ and ρ_c/ρ_∞=2.0, were simulated for the normal injection cases.

Inclined Injection

Fig. 2 depicts the averaged effectiveness predictions for M=0.5, 1.0 and 2.0 against the experimental data of references [9] and [10]. The numerical predictions of Demuren et al [7] for a hole spacing s/D of 3, but α of 45° are included in the figure. The three-dimensional partial differential equations governing the flow and temperature distributions in [7] were solved with a locally elliptic finite volume technique developed by Rodi and Srivatsa [16], the turbulent stresses and heat fluxes were evaluated with the nonisotropic version of the k-ε model proposed by Bergeles et al [4], and the wall function approach described in Launder and Spalding [14] was adopted. The general trend of the $\bar{\eta}$ development is predicted correctly in all cases. Furthermore, halving the grid size has produced negligible change in the predicted effectiveness indicating the independence of the predictions of grid size. The agreement with the measurements is seen to be best for the unity blowing rate, but for the highest blowing rate, $\bar{\eta}$ is underpredicted by as much as 30% downstream of x/D=10. Note that the values of $\bar{\eta}$ are generally small which compound the error. The effectiveness level predicted by Demuren et al [7] is observed

to follow the measurements better for M=0.5 and 2.0, although there is a difference in the angle of injection. However, the enhancement of the nonisotropic variant in the k-ε turbulence model in [7] probably has improved their $\bar{\eta}$ predictions.

In Fig. 3, Goldstein et al [9] effectiveness data for M=0.5 are displayed with the predictions along four lateral positions. The general trend of the predicted η is in fairly good agreement with the measurements, although the lateral variation is seen to be higher along the centreline and considerably lower in between the holes.

Normal Injection

The general picture of the lateral average effectiveness for the case of normal injection as predicted by the calculation scheme is much the same as for inclined injection as shown in Fig. 4. The initial behaviour, however, is less well predicted; differences with measurements up to 30% are observed. The farfield behaviour is fairly well predicted. The measurements in the figure are those of Foster [11] at a jet-to-mainstream density ratio of 2.0. The predictions of Demuren et al [7] for normal injection at unity density ratio are also shown. The prediction of Demuren et al are seen to be of the same manner as those predicted by Phoenics, but at M=1 the level of $\bar{\eta}$ as predicted by [7] is seen to be lower than the measurements presumably caused by the lower density of the jets.

Figs. 5(a) and (b) compare predicted and measured [11] lateral distribution and centreline effectiveness respectively for normal injection at density ratio of 2.0 for different blowing rates. It can be seen that the predicted effectiveness is higher than the measurements at centreline positions and appreciably lower in between the holes as has been observed for the case of 35° injection (Fig. 3). Nevertheless, the trends agree reasonably well with the measurements.

CONCLUSIONS

The computer code Phoenics has been applied to simulate the effects of film cooling by a row of holes over a flat surface.

The overall predicted level of laterally averaged effectiveness, $\bar{\eta}$, for both 90° and 35° holes was in fairly good agreement with experiment. The predictions were generally little lower than measurements, although maximum differences of 30% close to a hole were observed at some cases.

The predicted lateral distribution of effectiveness was found to be higher than measurements at centreline locations and considerably lower at mid-pitch positions for both 90° and 35° holes.

In general, the overall performance of the computer code Phoenics is shown to agree reasonably well with the effectiveness measurements, however, one should keep in mind that all of the cases examined lay in the strong injection regime where strong jet-mainstream mixing took place behind a hole.

NOMENCLATURE

c	concentration
c'	instantaneous concentration fluctuations about the mean
C_1, C_2, σ_k, σ_ε	empirical constants in turbulence model
C_f	skin-friction factor
D	injection hole diameter
E	constant for the law of the wall
k	kinetic energy of turbulence

k_v	Von Karman constant
M	blowing rate (mass flux ratio=$\rho_c u_c/\rho_\infty u_\infty$)
P	pressure
Re	Reynolds number
s	distance between centres of injection holes
T	temperature
Tu	turbulence intensity
u	velocity component in x-direction
u'	instantaneous velocity fluctuations about the mean
u_τ	friction velocity
w	velocity component in z-direction
x,y,z	Cartesian coordinates
α	injection inclination to the streamwise direction
δ	thickness of boundary layer
δ^*	boundary layer displacement thickness
Γ	diffusivity
ε	dissipation rate of turbulence
η	effectiveness
$\bar{\eta}$	lateral average effectiveness
$\hat{\eta}$	centreline effectiveness
μ	viscosity
ν	kinematic viscosity
ρ	density
τ	shear stress

Subscript

aw	adiabatic wall
c	coolant
D	injection hole diameter
eff	effective
iw	impermeable wall
l	laminar
t	turbulent
w	wall
∞	mainstream

REFERENCES

[1] Colladay, R. S. and Russell, L. M., "Streakline Flow Visualization of Discrete Hole Film Cooling for Gas Turbine Applications," ASME J. of Heat Transfer, May 1976, pp. 245-250.

[2] Patankar, S.V., Basu, D.K. and Alpay, S.A., "Prediction of the Three-Dimensional Velocity Field of a Deflected Turbulent Jet," ASME, J. of Fluids Engineering, Vol. 15, 1977, pp. 758-762.

[3] Bergeles, G., Gosman, A.D. and Launder, B.E., "The Prediction of Three-Dimensional Discrete-Hole Cooling Processes, Part 1: Laminar Flow," ASME, J. of Eng. for Power, 1976, pp. 379-386.

[4] Bergeles, G., Gosman, A.D. and Launder, B.E., "Double-Row Discrete-Hole Cooling: An Experimental and Numerical Study," ASME, J. of Eng. for Power, Vol. 102, 1980, pp. 498-503.

[5] Bergeles, G., Gosman, A.D. and Launder, B.E., "The Prediction of Three-Dimensional Discrete-Hole Cooling Processes, Part 2: Turbulent Flow," ASME, J. of Heat Transfer, Vol. 103, 1981, pp.141-145.

[6] Miller, K.L. and Crawford, M.E., "Numerical Simulation of Single, Double and Multiple Row Film Cooling Effectiveness and Heat Transfer," ASME 84-GT-112, 1984.

[7] Demuren, A.O., Rodi, W. and Schonung, B., "Systematic Study of Film Cooling with a Three-Dimensional Calculation Procedure," ASME, J. of Turbomachinery, Vol. 108, 1986, pp. 124-130.

[8] Tafti, D.K. and Yavuzkurt, S., "Prediction of Heat Transfer Characteristics for Discrete Hole Film Cooling - One Row Injection into a Turbulent Boundary Layer," presented at the ASME Winter Annual Meeting, Chicago, Nov. 1988.

[9] Goldstein, R.J., Eckert, E.R.G., Eriksen, V.L. and Ramsey, J.W., "Film Cooling Following Injection Through Inclined Circular Tubes," NASA CR-72612, 1969.

[10] Pedersen, D. R., Eckert, E. R. and Goldstein, R. J., "Film Cooling with Large Density Differences Between the Mainstream and the Secondary Fluid Measured by the Heat Mass Transfer Analogy," ASME J. of Heat Transfer, Vol. 99, 1977, pp. 620-627.

[11] Foster, N.W., "Film Cooling of Gas Turbine Blades," PhD Thesis, University of Nottingham, 1976.

[12] Rosten, H.I. and Spalding, D.B., "The PHOENICS Reference Manual," CHAM TR/200, Document Revision 06, Software Version 1.4, 1987.

[13] Rosten, H.I. and Spalding, D.B., "The PHOENICS Beginner's Guide," CHAM TR/100, Document Revision 04, Software Version 1.4, 1987.

[14] Launder, B.E. and Spalding, D.B., "The Numerical Computation of Turbulent Flows," Computer Methods in Applied Mechanics and Engineering, Vol. 3, 1974, pp. 269-289.

[15] Nagano, Y. and Hishida, M., "Improved Form of the K-E Model for Wall Turbulent Shear Flows," ASME, J. of Fluids Engineering, Vol. 109, 1987, pp. 156-160.

[16] Rodi, W. and Srivatsa, S.K., "A Locally Elliptic Calculation Procedure for Three-Dimensional Flows and Its Application to a Jet in Cross Flow," Comp. Meth. Appl. Mech. Engg., Vol. 23, 1980, pp. 67-83.

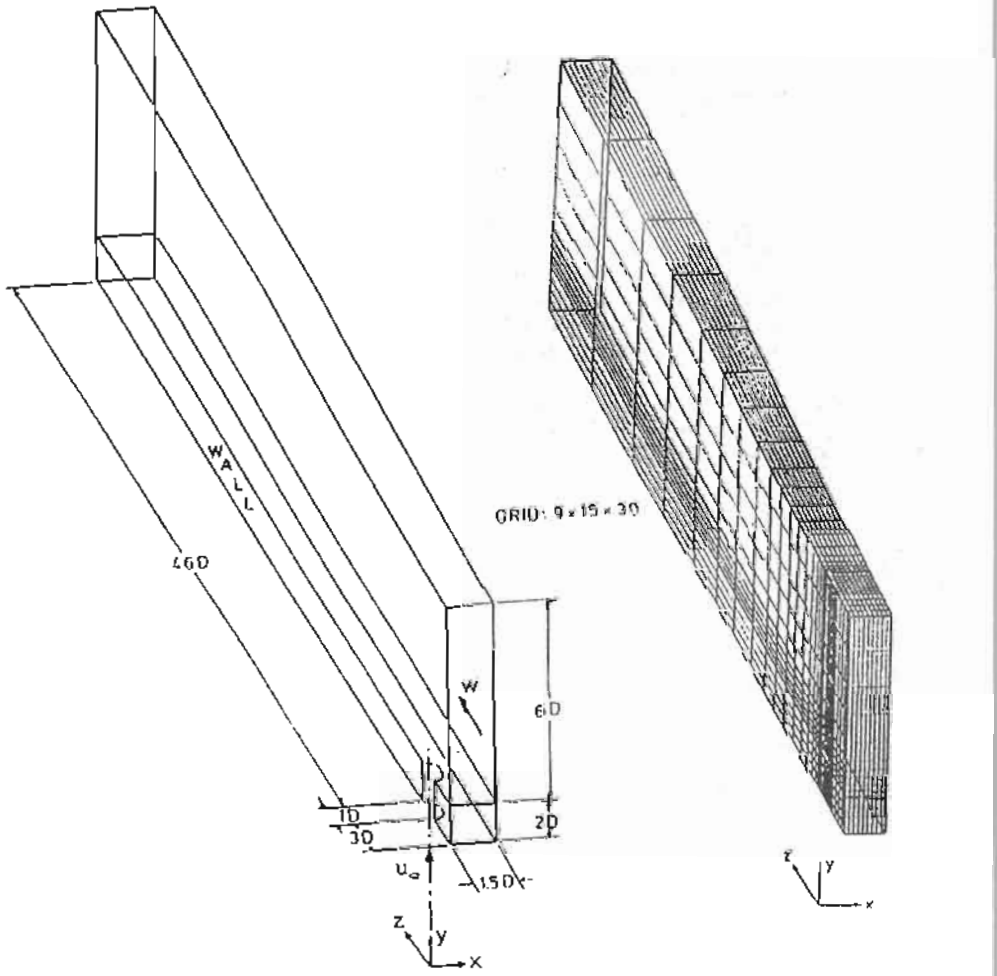

Fig. 1 Geometry and grid used.

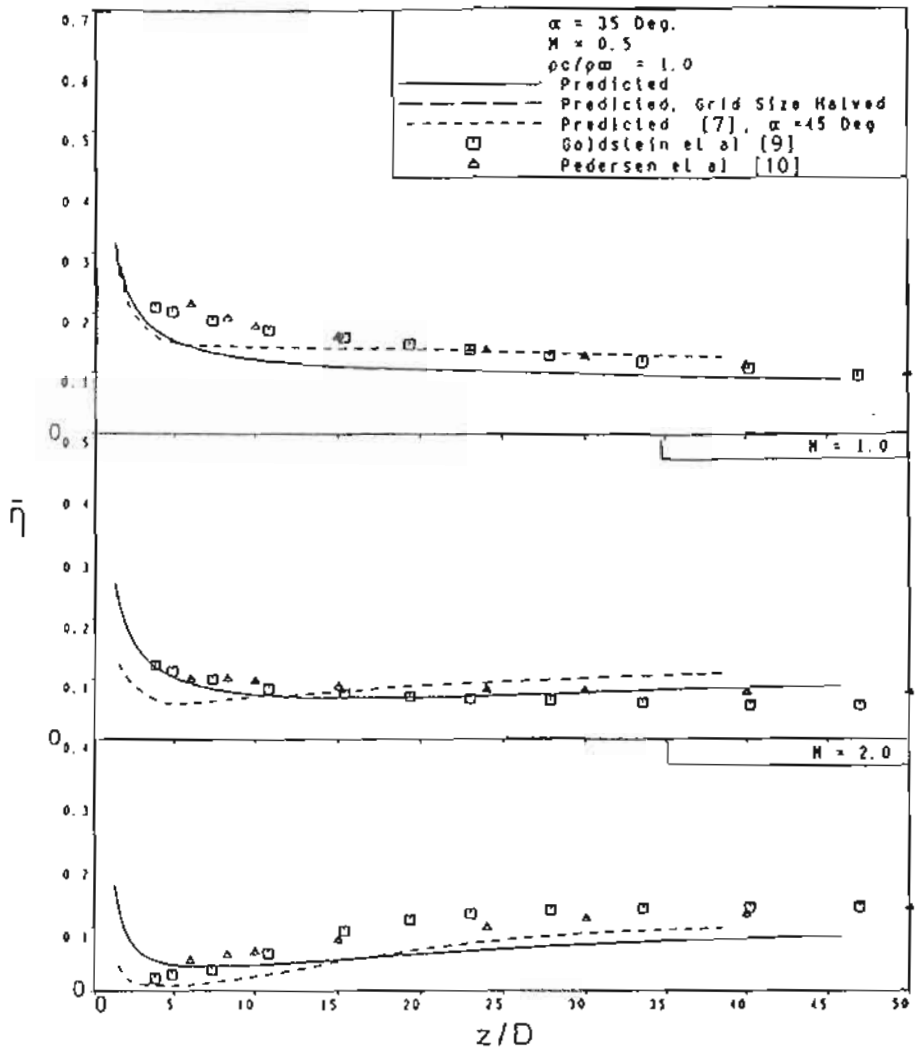

Fig. 2 Comparison between predicted and measured laterally averaged effectiveness following injection through a row of holes.

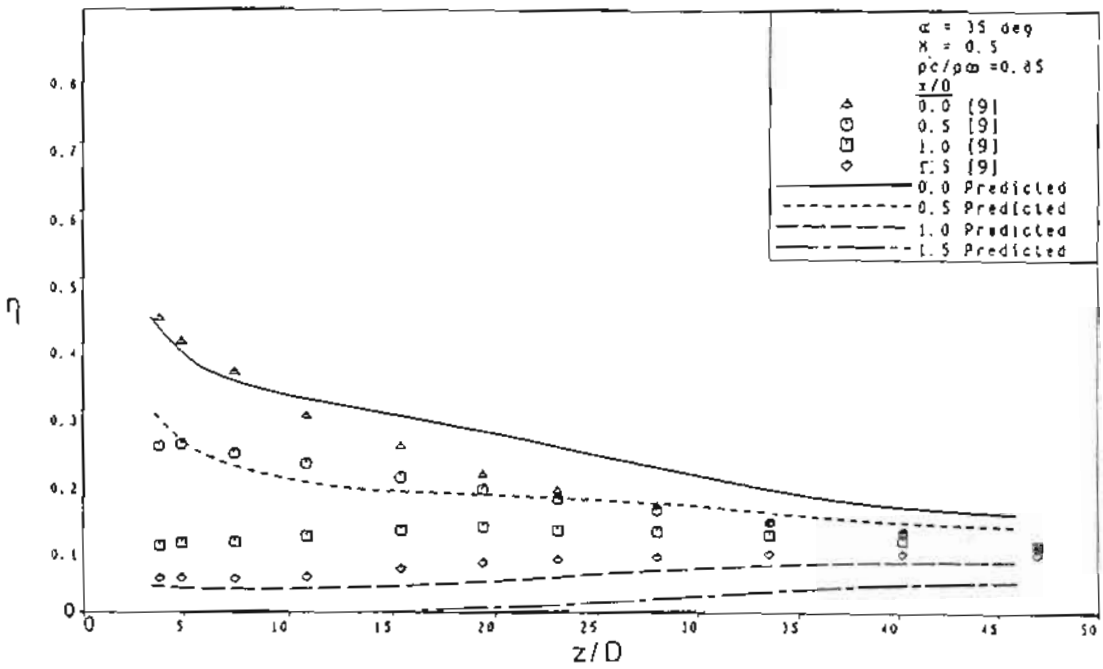

Fig. 3 Comparison between predicted and measured effectiveness following injection through a row of holes.

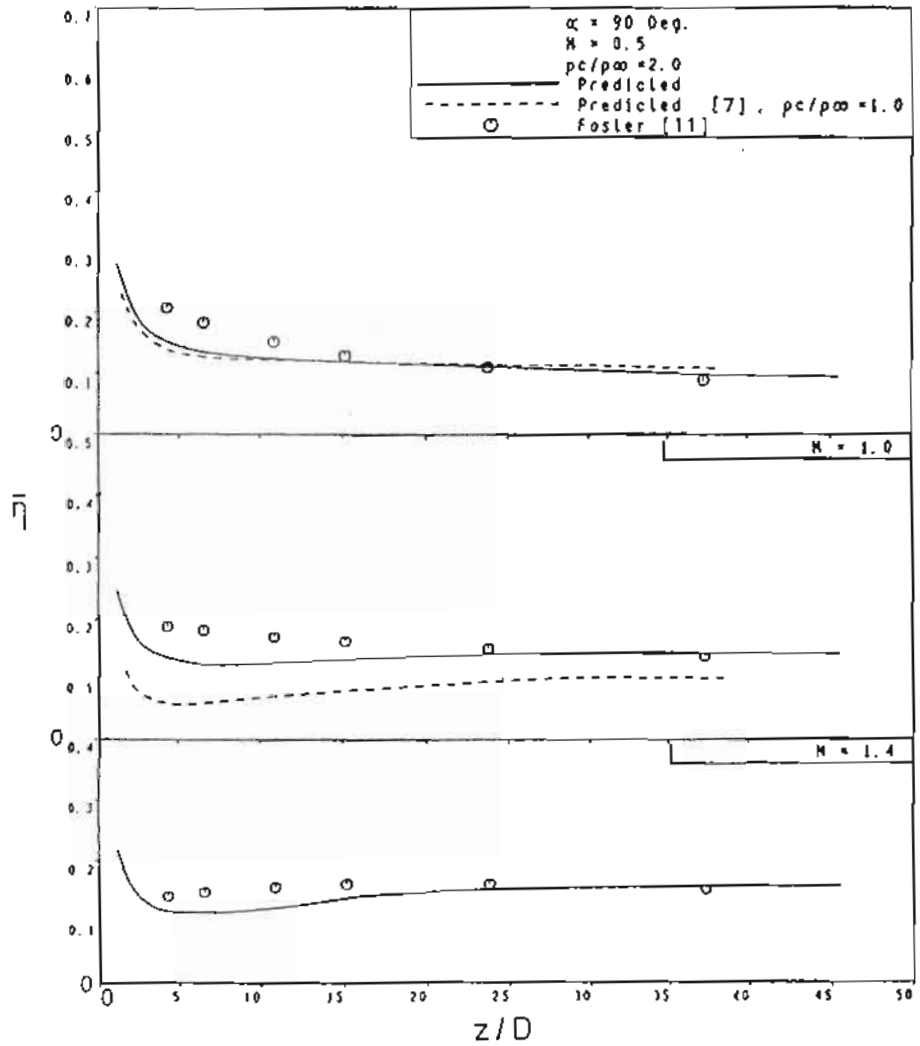

Fig. 4 Comparison between predicted and measured laterally averaged effectiveness following injection through a row of holes.

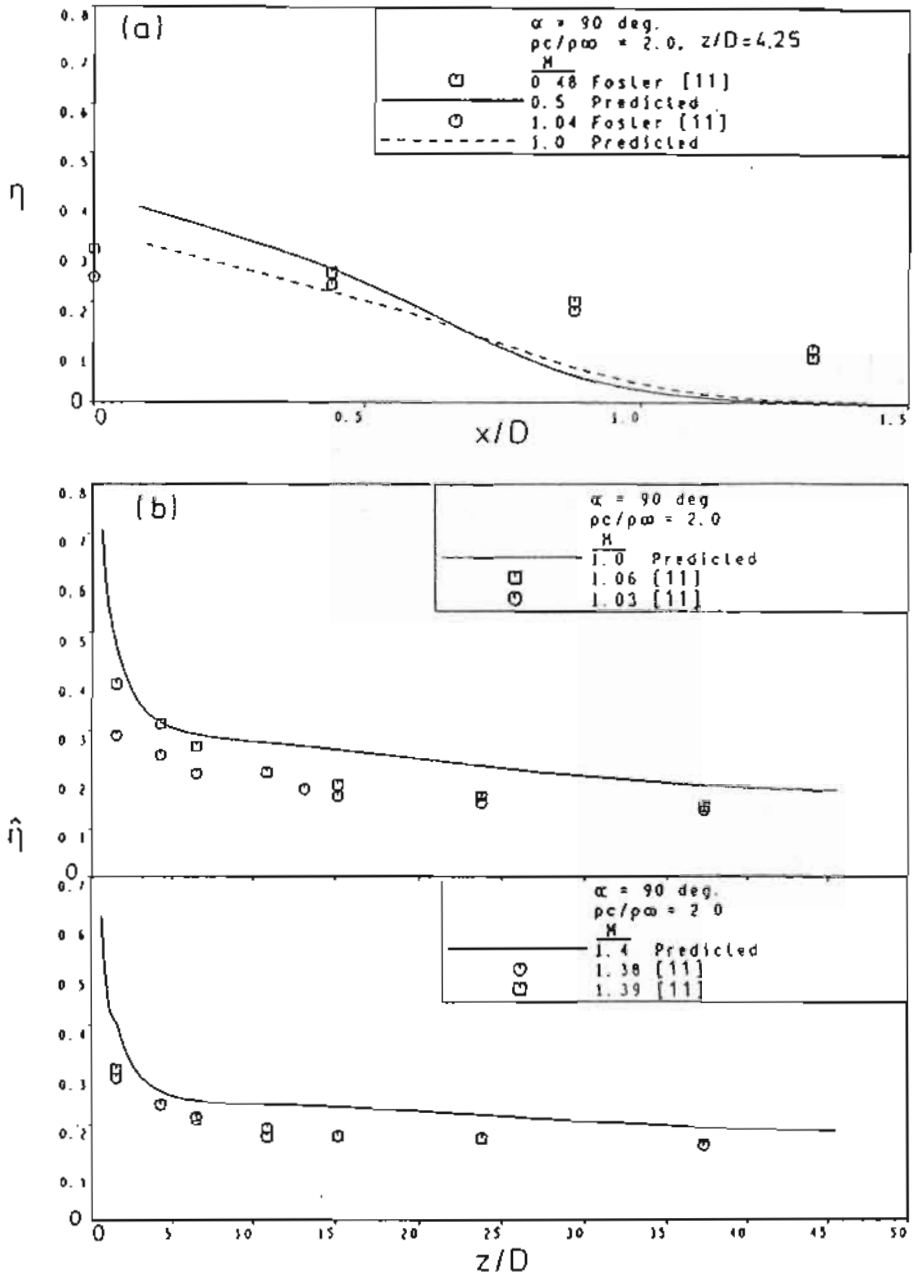

Fig. 5 Comparison between predicted and measured effectiveness following injection through a row of holes.